Inorg. Chem. **1990**, *29*, 3529-3538 **3529**

Contribution from the Department of Chemistry,
University of New Brunswick, Fredericton, New Brunswick, Canada E3B 6E2

Preparations and Crystal Structures of $Se_2I_4(AsF_6)_2{\cdot}SO_2$ and $Se_2I_4(Sb_2F_{11})_2$ and Electronic Structure of the Eclipsed Diselenium Tetraiodide Dication, Containing Two $SeI_2^{\cdot+}$ Radical Cations Joined via a $\pi^*-\pi^*$ Bond and a Delocalized $4p\pi-5p\pi$ Bond. Implications for Bonding in $S_2O_4^{2-}$, Se_8^{2+}, and S_8^{2+}

W. A. Shantha Nandana, Jack Passmore,* Peter S. White,* and Chi-Ming Wong

Received December 14, 1989

$Se_2I_4(AsF_6)_2{\cdot}SO_2$ and $Se_2I_4(Sb_2F_{11})_2$ were prepared quantitatively by reacting stoichiometric amounts of Se, I_2, and AsF_5 and by reacting Se and $I_2Sb_2F_{11}$ in liquid SO_2, respectively. The ^{77}Se NMR spectra (−70 °C) of the salts in SO_2 solution indicated the presence of Se_4^{2+}, SeI_3^+, and an unidentified peak at 1345 ppm (referenced to neat $(CH_3)_2Se$ at room temperature). Crystal data for $Se_2I_4(AsF_6)_2{\cdot}SO_2$: monoclinic, space group $P2_1/c$, $a = 13.454\ (2)$ Å, $b = 9.930\ (1)$ Å, $c = 14.576\ (1)$ Å, $\beta = 93.20\ (1)°$, $Z = 4$. $R = 0.043$ for 1045 significant reflections. Crystal data for $Se_2I_4(Sb_2F_{11})_2$: triclinic, space group $P\bar{1}$, $a = 17.915\ (1)$ Å, $b = 9.276\ (1)$ Å, $c = 8.001\ (1)$ Å, $\alpha = 96.04\ (1)°$, $\beta = 95.22\ (1)°$, $\gamma = 91.83\ (1)°$, $Z = 2$. $R = 0.046$ for 2647 significant reflections. The crystal packing of $Se_2I_4(AsF_6)_2{\cdot}2SO_2$ and $Se_2I_4(Sb_2F_{11})_2$ consists of columns of $Se_2I_4^{2+}$, AsF_6^-, and SO_2 and columns of $Se_2I_4^{2+}$ and $Sb_2F_{11}^-$, respectively. The $Se_2I_4^{2+}$ cations in both salts are similar and adopt the eclipsed configuration with long Se–Se bonds (average 2.841 (6) Å). There are significant intraionic interactions between the syn iodine atoms (average 3.673 (4) Å) that give the cation a distorted trigonal-prism-like shape. The Se–I bonds (average 2.451 (5) Å) are shorter than those in SeI_3^+ (average 2.510 (2) Å), implying $4p\pi-5p\pi$ bonding, with a formal bond order of 1.25 per Se–I bond. We conclude that $Se_2I_4^{2+}$ consists of two $SeI_2^{\cdot+}$ radical cations joined by a 6-center, 2-electron $\pi^*-\pi^*$ bond. This view is supported by ab initio (STO-3G) calculations on $S_2Cl_4^{2+}$ as a model for $Se_2I_4^{2+}$. The geometries of the related Se_8^{2+}, S_8^{2+}, and $S_2O_4^{2-}$ ions imply that they also contain similar $\pi^*-\pi^*$ bonds. The behavior of $Se_2I_4(AsF_6)_2$ and $Se_2I_4(Sb_2F_{11})_2$ in SO_2 solution is discussed.

Introduction

In the last 10 years, a large number of salts of sulfur–iodine and selenium–iodine cations have been prepared and characterized by single-crystal X-ray diffraction analyses in our laboratory. These include S_7IMF_6 (M = As, Sb),[1] $(S_7I)_2I(SbF_6)_3{\cdot}2AsF_3$,[2] $(S_7I)_4S_4(AsF_6)_6$,[2] $S_2I_4MF_6$,[3] SeI_3MF_6,[4] $Se_2I_4(Sb_2F_{11})_2$ (a preliminary report),[5] $(Se_6I)_n{\cdot}nMF_6$,[6] and $Se_6I_2(AsF_6)_2{\cdot}2SO_2$.[6] In addition, $Se_4I_4^{2+}$, $Se_6I_2^{2+}$, and SeI_3^+ cations were characterized in SO_2 solution at −80 °C by ^{77}Se NMR spectroscopy.[7] These cations are unexpectedly numerous, and they have unusual geometries that imply novel bonding situations. However, neutral sulfur iodides SI_2[8] and S_2I_2[9,10] have only been observed at low temperatures (−246 and −90 °C, respectively) and neutral binary selenium iodides have not been characterized,[11] although salts of SeI_6^{2-} have been known for some time.[12]

The novel $S_2I_4^{2+}$ cation in $S_2I_4(MF_6)_2$ (M = As, Sb)[3] is formally a salt of nonexistent I_3SSI_3. It was the first reported example of a hexaatomic species whose structure approximates that of a distorted right triangular prism and has sulfur–sulfur and iodine–iodine bond lengths indicative of bond orders 2.33 and 1.33, respectively. The cation may be regarded as consisting of $S_2^{0.66+}$ and two $I_2^{0.66+}$ units, weakly bonded together by electrons in π^* orbitals. Thus, π bonding in each dimer unit is maximized. The bonding situation may arise from the near equality of the ionization energies (IE's) of S_2 [9.36 (2) eV] and I_2 [9.3995 (12) eV].[13] To explore this hypothesis, the selenium analogue, $Se_2I_4^{2+}$ [IE = Se_2 8.88 (3) eV],[13] as the $Sb_2F_{11}^-$ and AsF_6^- salts, was prepared, and the structures of these salts were determined.

The $Se_2I_4^{2+}$ cations in $Sb_2F_{11}^-$ and AsF_6^- salts have very similar distorted trigonal-prismatic structures. The geometry of $Se_2I_4^{2+}$ is different from that of $S_2I_4^{2+}$ and isovalent P_2I_4[14] but similar to that of the $S_2O_4^{2-}$ anion[15,16] in that both ions are eclipsed and have long chalcogen–chalcogen bonds. We interpret the structure of the eclipsed $Se_2I_4^{2+}$ ion as arising from two $SeI_2^{\cdot+}$ radical cations, each containing a net one-half of a $4p\pi-5p\pi$ bond joined by a 6-center, 2-electron $\pi^*-\pi^*$ bond. This model is supported by quantum-mechanical ab initio calculations on $S_2Cl_4^{2+}$ of suitable geometry, as a model for $Se_2I_4^{2+}$. Thus, both $S_2I_4^{2+}$ and $Se_2I_4^{2+}$ contain π-bonded fragments that are joined by $\pi^*-\pi^*$ bonds. The geometry of $Se_2I_4^{2+}$ is very similar to that of the selenium atoms in the transannular region of Se_8^{2+}, and we argue that Se_8^{2+} (as well as S_8^{2+}) and $S_2O_4^{2-}$ also contain similar $\pi^*-\pi^*$ bonds. The occurrence of thermodynamically stable $np\pi-np\pi$ ($n > 3$) bonds and a variety of $\pi^*-\pi^*$ bonds, including those in the homopolyatomic cations of groups 16 and 17, are discussed in ref 17b. Sulfur and selenium halogen cations have been the subject of a recent review.[17a] A preliminary account of $Se_2I_4(Sb_2F_{11})_2$ has been given,[5] and full reports of this and $Se_2I_4(AsF_6)_2{\cdot}SO_2$ are reported below.

---

(1) Passmore, J.; Sutherland, G. W.; Taylor, P.; Whidden, T. K.; White, P. S. *Inorg. Chem.* **1981**, *20*, 3839.

(2) Passmore, J.; Sutherland, G.; White, P. S. *Inorg. Chem.* **1982**, *21*, 2717.

(3) (a) Passmore, J.; Sutherland, G. W.; Whidden, T. K.; White, P. S. *J. Chem. Soc., Chem. Commun.* **1980**, 289. (b) Murchie, M. P. Ph.D. Thesis, UNB, 1986. (c) Grein, F.; Murchie, M. P.; Passmore, J.; Sutherland, G. W.; Tajik, M.; Whidden, T. K.; White, P. S. *Inorg. Chem.*, to be submitted for publication.

(4) Johnson, J. P.; Murchie, M. P.; Passmore, J.; Tajik, M.; White, P. S.; Wong, C.-M. *Can. J. Chem.* **1987**, *65*, 2744 and references therein.

(5) Nandana, W. A. S.; Passmore, J.; White, P. S.; Wong, C.-M. *J. Chem. Soc., Chem. Commun.* **1982**, 1098.

(6) Nandana, W. A. S.; Passmore, J.; White, P. S.; Wong, C.-M. *Inorg. Chem.* **1989**, *28*, 3320 and references therein.

(7) Carnell, M. M.; Grein, F.; Murchie, M. P.; Passmore, J.; Wong, C.-M. *J. Chem. Soc., Chem. Commun.* **1986**, 225.

(8) Feuerhahn, M.; Vahl, G. *Inorg. Nucl. Chem. Lett.* **1980**, *16*, 5.

(9) Vahl, G.; Minkwitz, R. *Z. Anorg. Allg. Chem.* **1978**, *443*, 217.

(10) Manzel, K.; Minkwitz, R. *Z. Anorg. Allg. Chem.* **1978**, *441*, 165.

(11) *Gmelin Handbook of Inorganic Chemistry*, 8th ed.; Springer-Verlag: Berlin, 1984; Selenium (Suppl. Vol. B2).

(12) Greenwood, N. N.; Straughan, B. P. *J. Chem. Soc. A* **1966**, 962.

(13) Rosenstock, H. M.; Draxl, K.; Steiner, B. W.; Herron, J. T. *J. Phys. Chem. Ref. Data* **1977**, *6* (Suppl. 1).

(14) Leung, Y. C.; Waser, J. *J. Phys. Chem.* **1956**, *60*, 539.

(15) Dunitz, J. D. *Acta Crystallogr.* **1956**, *9*, 579.

(16) Kiers, C. Th.; Vos, A. *Acta Crystallogr.* **1978**, *B34*, 1499.

(17) (a) Passmore, J.; Klapötke, T. *Acc. Chem. Res.* **1989**, *22*, 234 and references therein. (b) Burford, N.; Passmore, J.; Sanders, J. C. P. In *From Atoms to Polymers, Isoelectronic Analogies*; Liebman, J. F., Greenberg, A., Eds.; Molecular Structure and Energetics, Vol. 8; Verlag Chemie: Deerfield Beach, FL, 1989; p 53. (c) Fujihara, H.; Akaishi, R.; Erata, T.; Furukawa, N. *J. Chem. Soc., Chem. Commun.* **1989**, 1789. (d) Fukihara, H.; Akaishi, R.; Furukawa, N. *J. Chem. Soc., Chem. Commun.* **1989**, 147 and references therein. Musker, W. K. *Acc. Chem. Res.* **1980**, *13*, 200 and references therein. (e) Iwasaki, F.; Toyoda, N.; Akaishi, R.; Fujihara, H.; Furukawa, N. *Bull. Chem. Soc. Jpn.* **1988**, *61*, 2563. (f) Alder, R. W.; Sessions, R. B.; Gmünder, J. O.; Grob, C. A. *J. Chem. Soc., Perkin Trans. 2* **1984**, 411. Nelsen, S. F.; Ippoliti, J. T. *J. Org. Chem.* **1986**, *51*, 3169. Musker, W. K.; Wolford, T. L.; Roush, P. B. *J. Am. Chem. Soc.* **1978**, *100*, 6416. Fujihara, H.; Chiu, J.-J. *J. Am. Chem. Soc.* **1988**, *110*, 1280.

0020-1669/90/1329-3529$02.50/0

Table I. Preparative Data for $Se_2I_4(AsF_6)_2{\cdot}SO_2$ and $Se_2I_4(AsF_6)_2$

reacn no.[a]	reactant wt, g			solvent wt, g		product wt, g	reacn time, days/pumping time in vacuo, h[c]	yield,[d] %		comments
	Se	I_2	AsF_5	SO_2	SO_2ClF[b]			Se_2I_4-$(AsF_6)_2{\cdot}SO_2$	Se_2I_4-$(AsF_6)_2$	
2(i)	1.022	3.290	3.502	7.05	1.28	7.438	7/0	104		one $Se_2I_4(AsF_6)_2{\cdot}SO_2$ crystal obtained
2(ii)[e]	0.531	1.702	1.752	7.41	1.99	3.870	20/<0.2	104		product largely one large crystal (ca. 0.5 cm^3), small fragments of which did not diffract well; elemental analysis of a portion of the crystal after pumping in vacuo for 12 h $SeI_{1.96}As_{1.00}F_{5.8}$
2(iii)[e]	0.669	2.147	2.270	5.88	2.61	4.898	40/0	104		crystalline material stored under gaseous SO_2 at 200 Torr prior to mounting of the crystals in the drybox; crystals did not diffract well
2(iv)[e]	0.520	1.650	3.56	4.76	4.10	3.65	3/<0.2	100		weight of the product suggested excess AsF_5 (ca. 100%) did not oxidize $Se_2I_4(AsF_6)_2{\cdot}SO_2$ any further; large crystal (ca. 0.75 cm^3) obtained, small fragments of which did not diffract well
3(i)	1.139	3.725	3.691	9.1		7.541	4/16		100	one "tetragonal phase" crystal isolated[f]
3(ii)[e]	1.443	4.628	4.658	10.0		10.092	6/16		106	crystals did not diffract well; elemental analysis $SeI_{1.98}As_{1.02}F_{6.1}$
3(iii)[e]	0.490	1.563	1.579	7.4	1.1	3.132	9/16		97	one "tetragonal phase" crystal isolated[f]

[a] Refer to numbered parts of the Experimental Section. [b] SO_2ClF was added to the solution which contained non insoluble material, after the reaction was completed. [c] After the volatile materials were removed, the products were subjected to dynamic vacuum for the time indicated. [d] Based on Se as the limiting reagent. [e] Data included here are for experiments similar to those described in the text. [f] Cell parameters: a = 11.139 (9), c = 23.925 (11) Å; tetragonal; space group $P4_122$.

$Se_2I_4^{2+}$ and $S_2I_4^{2+}$ are the only known examples of (chalcogen)$_2$(halogen)$_4^{2+}$ dications. There appear to be no other examples of $Se_2R_4^{2+}$ (R = univalent group) except the 1,5-diselenacyclooctane dication (**1a**), the preparations of which has been recently reported.[17c] Studies of $S_2R_4^{2+}$ (R = organic univalent group) are more extensive,[17d] although the only structural determination is that of the sulfur analogue[17e] of **1a**, i.e. **1b**. The S–S distance in **1b** is 2.124 (3) Å (average); i.e. it is a normal S–S bond with some lengthening, presumably due to electrostatic and bond/bond, lone pair/lone pair repulsions. Thus the chalcogen bond in **1b** is very different from that in $Se_2I_4^{2+}$. $Se_2I_4^{2+}$ is formally a relatively rare example of a general class of dication, containing two bonded positively charged atoms of the same element (e.g. **1a**, **1b**, $\gt N^+–N^+\lt$), that is of considerable current interest.[17f]

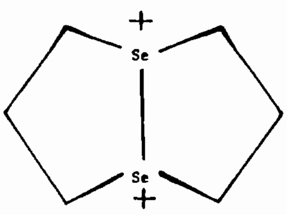

1a

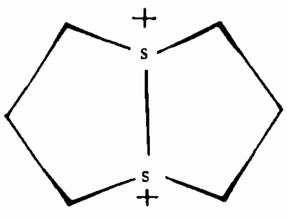

1b

Experimental Section

Apparatus and techniques used in this work have been described.[18-20] Reactions were carried out in a two-bulb Pyrex glass vessel equipped with a J. Young Teflon-stemmed glass valve and a coarse sintered-glass frit. Elemental selenium (BDH), iodine (BDH), and AsF_5 (Ozark-Mahoning) were used without further purification. $I_2Sb_2F_{11}$ was prepared by our published procedure.[20] SO_2ClF (Aldrich) was distilled onto and stored over CaH_2. Solutions were prepared in 10-mm-o.d., thick-walled (1 mm) NMR tubes (Wilmad Glass Co., Buena, NJ) joined to Teflon-in-glass valves (J. Young, O-ring PTFE stopcock) for NMR spectroscopic measurements.

^{77}Se NMR spectra were recorded unlocked with a Varian XL-200 spectrometer equipped with a variable-temperature controller and a 10-mm probe (broad-banded over the frequency range 20–125 MHz) tuned to 38.164 MHz by using 32K of memory and a spectral width of 50 kHz (3.2 Hz/data point; pulse repetition time 0.32 s) and a pulse width of 12 μs. ^{19}F NMR spectra were obtained on the same probe by using the ^{1}H decoupler, retuned to 188.220 MHz, as the observe coil and a pulse width of 6 μs.

Infrared spectra of solids were obtained as fine powders between KBr or AgCl plates by using a Perkin-Elmer Model 683 spectrometer.

1. Preparation of $Se_2I_4(Sb_2F_{11})_2$. (i) In a typical reaction, a solution of $I_2Sb_2F_{11}$ (6.043 g, 8.60 mmol, in 10.1 g of liquid SO_2) was poured onto Se (0.558 g, 7.07 mmol) in the second bulb of a two-bulb vessel.[18] The color of the solution changed immediately from blue to dark brown-red, and after 2 days no solid remained. The solvent was slowly condensed over to the other bulb. After 16 h, some dark microcrystalline material formed under the solution. The supernatant solution was filtered into the second bulb, and the volatile materials were removed by evacuation under dynamic vacuum for 1 h. The crystalline product was dark brown-black, but small fragments appeared to be red. Several crystals were identified as $Se_2I_4(Sb_2F_{11})_2$ by X-ray crystallography.

(ii) A solution of $I_2Sb_2F_{11}$ (5.282 g, 7.48 mmol, in 12.6 g of liquid SO_2) was poured onto Se (0.594 g, 7.52 mmol), giving a homogeneous dark brown-red solution containing no solid after 3 days. SO_2ClF (2.1 g) was condensed onto the solution, and some dark microcrystalline material precipitated immediately. The solvent was removed by evacuation, giving 2.996 g of solid. IR (cm^{-1}): 772 w, sh, 740 w, sh, 728 s, sh, 712 w, sh, 680 s, sh, 655 s, 620 w, sh, 585 w, sh, 572 w, 487 m. Anal. Calcd for $SeI_2Sb_2F_{11}$: Se, 10.06; I, 32.32; Sb, 31.01; F, 26.6. Found: Se, 9.86; I, 31.41; Sb, 32.49;, F, 26.8.

2. Preparation of Crystalline $Se_2I_4(AsF_6)_2{\cdot}SO_2$ (i). In a typical reaction, SO_2 (7.05 g) and AsF_5 (3.502 g, 20.61 mmol) were condensed onto Se (1.022 g, 12.94 mmol) and I_2 (3.290 g, 12.96 mol). A dark brown-red solution formed immediately, and after 16 h no insoluble material was observed. SO_2ClF (1.28 g) was condensed onto the solution, leading to the immediate formation of some dark crystalline material. The solvent was slowly (ca. 20 h) condensed over to the other bulb by cooling it with running cold tap water (10 °C). A large amount of dark brown-black crystalline material was formed. The crystals were washed twice with ca. 1 mL of the solvent. After all the volatile materials were removed by evacuation, the shiny surfaces of the crystals (total 7.438 g) rapidly turned dull without any observable color change, and therefore the evacuation was stopped. Seven crystals were quickly mounted in Pyrex capillaries. Only one of the crystals diffracted X-rays sufficiently well for X-ray diffraction studies and was subsequently identified as $Se_2I_4(AsF_6)_2{\cdot}SO_2$. The results from similar experiments (reactions 2-(ii)–2(iv)) are summarized in Table I.

3. Preparation of $Se_2I_4(AsF_6)_2$ (ii). In one reaction, AsF_5 (3.691 g, 21.73 mmol) was condensed onto a mixture of Se (1.139 g, 14.42 mmol) and iodine (3.725 g, 14.67 mmol) in liquid SO_2 (9.1 g). An immediate reaction took place, resulting in a dark brown-red solution with no solid material. The solvent was slowly (ca. 20 h) condensed into the second bulb, leading to the formation of some dark crystalline material, and after 16 h was evacuated, giving 7.541 g of solid product. Only one among several of the crystals examined was suitable for X-ray diffraction studies. Crystal data: a = 11.139 (9), c = 23.925 (11) Å; tetragonal; space group

---

(18) Murchie, M. P.; Passmore, J. *Inorg. Synth.* **1986**, *24*, 76.
(19) Passmore, J.; Taylor, P. *J. Chem. Soc., Dalton Trans.* **1976**, 804.
(20) Passmore, J.; Richardson, E. K.; Taylor, P. *J. Chem. Soc., Dalton Trans.* **1976**, 1006. Apblett, A.; Green, F.; Johnson, J. P.; Passmore, J.; White, P. S. *Inorg. Chem.* **1986**, *25*, 422.

$P4_122$. We refer to crystals with these cell parameters as the "tetragonal phase".

The results from similar experiments (reactions 3(ii) and 3(iii)) are summarized in Table I.

Properties of Solid $Se_2I_4(AsF_6)\cdot SO_2$. The shiny surfaces of the dark brown-black $Se_2I_4(AsF_6)_2\cdot SO_2$ crystals rapidly become dull under a dynamic vacuum and on manipulation in the drybox, but retain their shiny surfaces under 200 mmHg of SO_2 (reaction 2(iii)). When the $Se_2I_4(AsF_6)_2\cdot SO_2$ crystals are subjected to a dynamic vacuum for ca. 16 h, the SO_2 is removed quantitatively. Brown-black crystalline $Se_2I_4(AsF_6)_2\cdot SO_2$ becomes a reddish brown powder upon grinding. IR (cm^{-1}): 655 s, 550 m.

$Se_2I_4(AsF_6)_2$ and $Se_2I_4(Sb_2F_{11})_2$ in SO_2 Solution. A homogeneous appearing dark red solution of $Se_2I_4(AsF_6)_2$ (0.497 g, 0.477 mmol) in SO_2 (3.94 g) was cooled to −10 °C, leading to the formation of some yellow solid that readily redissolved at room temperature with agitation. The solution was cooled to −50 °C for 15 min and warmed to room temperature without agitation. The supernatant solution was decanted into a second bulb, and the precipitate was washed twice with ca. 1 mL of solvent. The yellow precipitate was identified as $Se_4(AsF_6)_2$ (0.018 g) by Raman spectroscopy.[21] SO_2ClF (1.2 g) was condensed onto the supernatant solution in the other bulb, and the solvent was slowly removed over a period of 5 h, leading to crystalline SeI_3AsF_6, identified by single-crystal X-ray diffraction.[4] The formation of a yellow precipitate, $Se_4(AsF_6)_2$, at low temperature (<−10 °C) was also observed in $Se_2I_4(AsF_6)$ solutions prepared in situ.

The ^{77}Se NMR spectra (−70 °C) obtained from the $Se_2I_4(AsF_6)_2$ solution prepared in situ (0.348 g of Se, 1.104 g of I_2, and 1.120 g of AsF_5 in 5.16 g of liquid SO_2) and from redissolving $Se_2I_4(AsF_6)_2$ in liquid SO_2 (0.38 M) showed three peaks at 1923, 1345, and 833 ppm (referenced to neat $(CH_3)_2Se$ at room temperature) with peak widths of 4–8 Hz and relative integrated areas of ca. 1:11:9 and relaxation times of all less than 0.5 s. The peaks at 1923 and 833 ppm can be assigned to $Se_4{}^{2+}$[22] and $SeI_3{}^+$,[7] respectively, but the peak at 1345 ppm is yet unassigned with certainty. Addition of excess AsF_5 (150% with respect to eq 2) to the $Se_2I_4(AsF_6)_2$ solution changed the relative integrated areas of the three peaks at 1923, 1345, and 833 ppm to 1:4:3. The ^{77}Se NMR spectrum (−80 °C) obtained by redissolving $Se_2I_4(Sb_2F_{11})_2$ (0.4 M) in SO_2 also showed three peaks at 1922 ($Se_4{}^{2+}$), 1339 (unassigned), and 833 ppm ($SeI_3{}^+$) with relative integrated areas of ca. 1:2:1.

The ^{19}F NMR spectrum (−70 °C) of $Se_2I_4(AsF_6)_2$ indicated the presence of $AsF_6{}^-$.[23] The ^{19}F NMR spectrum (−80 °C) of $Se_2I_4(Sb_2F_{11})_2$ showed the presence of largely $Sb_2F_{11}{}^-$ (−90, −109, and −131 ppm referenced to neat CCl_3F at room temperature; relative integrated areas 1:8:2)[24] and its equilibrium product $SbF_5\cdot SO_2$ (−99 ppm, ca. 5% of the total integrated area in the spectrum).[24]

The ^{77}Se NMR spectrum (−70 °C) of $Se_2I_4(AsF_6)_2$ (0.313 g, 3.00 mmol) and I_2 (0.079 g, 3.1 mmol) in liquid SO_2 (3.99 g) contained only one peak at 834 ppm, similar to that of pure SeI_3AsF_6 in SO_2 solution.[7]

X-ray Crystallographic Analysis. $Se_2I_4(Sb_2F_{11})_2$. Diffraction intensities were measured on a Picker FACS-1 diffractometer, equipped with graphite-monochromated Mo Kα radiation and running the NRC Picker control program. The ω–2θ scans were used with a profile analysis in order to improve the background estimates. Unit cell parameters were obtained by a least-squares fit to the centered coordinates of 25 reflections and their Friedel opposites. Lorentz and polarization factors were applied and absorption corrections were made by using the empirical routine of Stuart and Walker.[25]

$Se_2I_4(AsF_6)_2\cdot SO_2$. Diffraction intensities were measured on an Enraf-Nonius CAD-4 diffractometer, equipped with graphite-monochromated Mo Kα radiation and running the NRCCAD[26] control program. An ω–2θ scan was used at a speed of 4° (2θ) min^{-1}; backgrounds were estimated by extending the scan by 25% on either side of the scan limits. The limits of the peak were then ascertained by profile analysis to provide an improved background correction. Unit cell parameters were obtained by least-squares refinement using the coordinates of 25 reflections centered by using the TRUANG option of NRCCAD, thereby minimizing the effects of instrumental and crystal alignment errors. Lorentz and polarization factors were applied and absorption corrections were made by using the empirical routine of Stuart and Walker.[25]

Table II. Crystal Data for $Se_2I_4(Sb_2F_{11})_2$ and $Se_2I_4(AsF_6)_2\cdot SO_2$

chem formula	$Se_2I_4(Sb_2F_{11})_2$	$Se_2I_4(AsF_6)_2\cdot SO_2$
fw	1570.1	1107.4
cryst syst	triclinic	monoclinic
space group	$P\bar{1}$ (2)	$P2_1/c$ (14)
a, Å	17.915 (2)	13.454 (2)
b, Å	9.276 (1)	9.930 (1)
c, Å	8.001 (1)	14.576 (1)
α, deg	96.04 (1)	
β, deg	95.22 (1)	93.20 (1)
γ, deg	91.83 (1)	
V, Å^3	1316.0 (4)	1944.3 (4)
Z	2	4
temp, °C	20	20
calcd density, g cm^{-3}	3.97	3.78
μ, cm^{-1}	116.2	103.0
λ, Å	0.7069	0.7069
transm coeff	0.157–0.291	0.073–0.198
R^a (including unobsd reflns)	0.0463 (0.0677)	0.043 (0.0163)
$R_w{}^b$ (including unobsd reflns)	0.0665 (0.0759)	0.041 (0.052)

$^a R = \sum|\Delta F|/\sum|F_o|$. $^b R_w = (\sum w|\Delta F|^2/\sum wF_o{}^2)^{1/2}$.

Table III. Atomic Positional Parameters (Fractional, ×10^4) for and Isotropic Thermal Parameters (Å^2) $Se_2I_4(Sb_2F_{11})_2$ (Estimated Standard Deviations in Parentheses)

atom	x/a	y/b	z/c	$B_{iso}{}^a$
Se(1)	2397.7 (9)	190.0 (17)	9734.5 (21)	2.95 (7)
Se(2)	2762.1 (9)	1608.2 (18)	13044.6 (21)	3.10 (6)
I(1)	3515.7 (7)	857.8 (13)	8390.8 (15)	3.92 (5)
I(2)	1410.3 (8)	1757.8 (17)	8819.4 (18)	5.52 (7)
I(3)	4016.0 (6)	2667.7 (13)	12792.2 (15)	3.76 (5)
I(4)	1924.0 (7)	3634.6 (15)	13044.8 (18)	5.00 (6)
Sb(1)	1117.9 (6)	8454.0 (12)	14008.6 (14)	3.16 (5)
Sb(2)	716.2 (7)	6319.3 (13)	17863.2 (15)	3.49 (5)
F(1)	1521 (7)	9341 (14)	12270 (15)	6.2 (6)
F(2)	199 (6)	7990 (13)	12809 (14)	5.3 (6)
F(3)	1445 (6)	6664 (11)	13314 (15)	5.2 (5)
F(4)	1994 (6)	8828 (15)	15448 (15)	6.0 (6)
F(5)	783 (8)	10203 (13)	14902 (17)	6.4 (6)
F(6)	682 (6)	7570 (13)	15894 (14)	5.2 (5)
F(7)	126 (9)	7705 (17)	18832 (18)	8.5 (8)
F(8)	1525 (8)	7486 (16)	18710 (18)	7.6 (7)
F(9)	1278 (9)	5114 (16)	16610 (19)	8.2 (8)
F(10)	−142 (7)	5420 (17)	16734 (19)	8.1 (8)
F(11)	794 (8)	5214 (16)	19659 (17)	7.4 (7)
Sb(3)	5903.3 (6)	2286.8 (12)	6876.8 (14)	3.07 (4)
Sb(4)	6328.5 (6)	4427.3 (12)	11449.2 (13)	2.94 (5)
F(21)	5860 (8)	1099 (15)	4888 (16)	6.9 (7)
F(22)	6719 (8)	3401 (16)	6495 (21)	8.0 (8)
F(23)	6533 (7)	1103 (13)	7968 (16)	6.0 (6)
F(24)	5105 (7)	1341 (14)	7621 (18)	7.4 (7)
F(25)	5266 (8)	3639 (15)	6059 (17)	7.4 (7)
F(26)	5944 (6)	3480 (11)	9095 (12)	4.7 (5)
F(27)	5666 (6)	5859 (11)	10946 (13)	4.5 (5)
F(28)	5534 (6)	3406 (13)	12153 (16)	5.6 (5)
F(29)	6898 (7)	2845 (12)	11595 (18)	6.4 (6)
F(30)	7058 (6)	5331 (12)	10379 (15)	5.2 (5)
F(31)	6682 (8)	5367 (15)	13541 (14)	6.9 (6)

$^a B_{iso}$ is the mean of the principal axes of the thermal ellipsoid.

Both structures were solved by using the direct methods technique and subsequent difference syntheses. Crystal data are summarized in Table II. Refinement was by full-matrix least squares with weights based on counter statistics. All atoms, with the exception of disordered fluorine atoms, were refined with anisotropic thermal parameters. All computations were performed by using the NRCVAX suite of crystal structure programs.[27] Scattering factors were taken from ref 28 and were corrected for anomalous dispersion. The final atomic coordinates are given in Tables III and IV; anisotropic thermal parameters and observed and calculated structure factors have been deposited as supplementary material.

---

(21) Burns, R. C.; Gillespie, R. J. *Inorg. Chem.* **1982**, *21*, 3877.

(22) Collins, M. J.; Gillespie, R. J.; Sawyer, J. F.; Schrobilgen, G. J. *Inorg. Chem.* **1986**, *25*, 2053.

(23) Dungan, C. H.; Van Wazer, J. R. *Compilation of Reported ^{19}F N.M.R. Chemical Shifts*; Wiley-Interscience: New York, 1970.

(24) Dean, P. A. W.; Bacon, J.; Gillespie, R. J. *Can. J. Chem.* **1969**, *47*, 1655.

(25) Walker, N.; Stuart, D. *Acta Crystallogr.* **1983**, *A39*, 158.

(26) Le Page, Y.; White, P. S.; Gabe, E. J. NRCCAD: An Enhanced CAD-4 Control Program. Presented at the Annual Meeting of the American Crystallographic Association, Hamilton, Ontario, Canada, 1986.

(27) Gabe, E. J.; Le Page, Y.; Charland, J.-P.; Lee, F. L.; White, P. S. *J. Appl. Crystallogr.* **1989**, *22*, 384.

(28) *International Tables for X-ray Crystallography*; Kynoch Press: Birmingham, England, 1974; Vol. IV.

Table IV. Atomic Positional Parameters (Fractional) and Isotropic Thermal Parameters (Å^2) for $Se_2I_4(AsF_6)_2{\cdot}SO_2$ (Estimated Standard Deviations in Parentheses)

atom[a]	x/a	y/b	z/c	B_{iso}[b]
Se(1)	0.2748 (3)	0.2142 (4)	0.69472 (23)	3.06 (19)
Se(2)	0.4069 (3)	0.1870 (4)	0.55055 (24)	3.46 (20)
I(1)	0.14167 (19)	0.06373 (25)	0.63667 (17)	3.78 (13)
I(2)	0.20974 (20)	0.4417 (3)	0.66307 (18)	4.30 (14)
I(3)	0.31506 (21)	0.0169 (3)	0.45698 (17)	4.49 (14)
I(4)	0.36728 (21)	0.3991 (3)	0.47003 (18)	4.79 (14)
S(1)	0.8501 (9)	0.2028 (11)	0.1204 (7)	5.6 (6)
O(1)	0.7731 (23)	0.145 (3)	0.0621 (21)	10.1 (22)
O(2)	0.8401 (21)	0.3410 (25)	0.1329 (17)	6.4 (16)
As(1)	0.9802 (3)	0.7230 (4)	0.61175 (25)	3.38 (20)
F(11)	0.973 (3)	0.662 (3)	0.5081 (15)	11.7 (21)
F(12)	0.8572 (15)	0.748 (3)	0.6034 (22)	11.1 (20)
F(13)	0.9902 (20)	0.7909 (25)	0.7181 (15)	8.8 (16)
F(14)	1.1070 (16)	0.705 (3)	0.6174 (16)	8.5 (16)
F(15)	0.9961 (16)	0.8809 (20)	0.5647 (13)	5.7 (12)
F(16)	0.9688 (17)	0.5674 (21)	0.6544 (16)	7.4 (15)
As(2)	0.5785 (3)	0.1805 (4)	0.26696 (25)	3.52 (19)
F(21)	0.596 (3)	0.020 (4)	0.311 (3)	5.2 (10)
F(22)	0.561 (4)	0.337 (5)	0.227 (3)	9.0 (15)
F(23)	0.454 (4)	0.164 (6)	0.269 (4)	10.5 (17)
F(24)	0.571 (3)	0.131 (5)	0.158 (3)	6.9 (12)
F(25)	0.597 (4)	0.240 (5)	0.378 (3)	9.5 (15)
F(26)	0.701 (4)	0.204 (6)	0.268 (4)	10.2 (16)
F(31)	0.483 (3)	0.117 (4)	0.194 (3)	6.1 (11)
F(32)	0.676 (4)	0.227 (5)	0.338 (3)	9.2 (15)
F(33)	0.497 (4)	0.280 (6)	0.307 (4)	10.6 (17)
F(34)	0.548 (3)	0.066 (4)	0.351 (3)	6.5 (12)
F(35)	0.648 (4)	0.060 (5)	0.221 (3)	8.2 (14)
F(36)	0.610 (3)	0.289 (4)	0.177 (3)	7.0 (12)

[a] F(21)–F(36) are disordered fluorine atoms with occupancies of 50%. [b] B_{iso} is the mean of the principal axes of the thermal ellipsoid.

Results and Discussion

Preparation of $Se_2I_4(Sb_2F_{11})_2$. Reaction between elemental selenium and $I_2Sb_2F_{11}$ in an approximately 1:1 mole ratio in SO_2 solution yielded single crystals of $Se_2I_4(Sb_2F_{11})_2$, which were characterized by single-crystal X-ray diffraction analyses. In another similar reaction the salt was prepared quantitatively according to eq 1, and the product was identified by full elemental

$$2Se + 2I_2Sb_2F_{11} \xrightarrow{SO_2} Se_2I_4(Sb_2F_{11})_2 \qquad (1)$$

analyses. The infrared spectrum of the solid[29,30] and the ^{19}F NMR spectrum of the SO_2 solution showed the presence of $Sb_2F_{11}^-$.[24]

Preparation of $Se_2I_4(AsF_6)_2{\cdot}SO_2$. The $Se_2I_4(AsF_6)_2{\cdot}SO_2$ salt was prepared essentially quantitatively in liquid SO_2 according to eq 2. It is important that the mole ratio of Se to I_2 is 1:1, since

$$2Se + 2I_2 + 3AsF_5 \xrightarrow{SO_2} Se_2I_4(AsF_6)_2{\cdot}SO_2 + AsF_3 \qquad (2)$$

the presence of excess iodine, with respect to eq 2, leads to the formation of SeI_3AsF_6 solid.[19] However, excess AsF_5 did not lead to any further oxidation (within a time period of 3 days, see reaction 2(iv) Table I).[31] Volatile materials, including excess AsF_5, were removed on evacuation under dynamic vacuum, leaving $Se_2I_4(AsF_6)_2{\cdot}SO_2$ as the crystalline product. In some reactions, the product weights were slightly greater than the calculated weights (Table I), probably due to the presence of a small quantity of excess SO_2 or AsF_3.

Only one single crystal of $Se_2I_4(AsF_6)_2{\cdot}SO_2$ that diffracted well has been isolated (i.e. reaction 2(i), Table I). Other attempts to prepare crystalline $Se_2I_4(AsF_6)_2{\cdot}SO_2$ did not yield crystalline material. The SO_2 in $Se_2I_4(AsF_6)_2{\cdot}SO_2$ is very labile. The shiny surfaces of the crystals rapidly became dull upon evacuation and very likely lost SO_2 during manipulation in the drybox with subsequent loss of crystallinity. The infrared spectrum of the ground $Se_2I_4(AsF_6)_2{\cdot}SO_2$ indicated the presence of AsF_6^- only.[32] The weights of the bulk products (reactions 3(ii) and 3(iii), Table I) showed that the SO_2 in $Se_2I_4(AsF_6)_2{\cdot}SO_2$ was removed quantitatively according to eq 3 on evacuation for ~16 h.

$$Se_2I_4(AsF_6)_2{\cdot}SO_2(cr) \xrightarrow{\text{in vacuo}} Se_2I_4(AsF_6)_2(s) + SO_2(g) \qquad (3)$$

It is therefore not surprising that single crystals of $Se_2I_4(AsF_6)_2{\cdot}SO_2$ were not isolated from reactions 3(i)–3(iii), Table I, since the bulk materials had been subjected to a dynamic vacuum for ~16 h. The labile nature of SO_2 in $Se_2I_4(AsF_6)_2{\cdot}SO_2$ is reminiscent of that in $Te_6(AsF_6)_4{\cdot}SO_2$[33] (see below and ref 36).

Large crystals of $Se_2I_4(AsF_6)_2{\cdot}SO_2$ (0.5–0.75 cm^3, reactions 2(ii) and 2(iv), Table I) were obtained from $Se_2I_4(AsF_6)_2$ solutions that contained no insoluble material prior to crystal growth. Although fragments of the large crystal did not diffract X-rays, elemental analyses of the large crystal after evacuation for 16 h (eq 3) were consistent with the formulation of $Se_2I_4(AsF_6)_2$ (reaction 2(ii), Table I). Thus, the weights of the bulk products, the formation and the elemental analyses of the large crystal, and the isolation of a single crystal of $Se_2I_4(AsF_6)_2{\cdot}SO_2$ were consistent with the bulk product having the formulation $Se_2I_4(AsF_6)_2{\cdot}SO_2$ prior to evacuation.

Nature of the "Tetragonal Phase". Two single crystals of the tetragonal phase were isolated from three reactions (reactions 3(i)–3(iii), Table I) out of a total of 25 crystals examined. Presumably, the amorphous "solid" was $Se_2I_4(AsF_6)_2$. Of 35 other "crystals" examined from a number of other reactions (reactions 2(i)–2(iv), Table I), none were of the tetragonal phase.

It is possible that the bulk material is not completely pure. However, it must be almost all $Se_2I_4(AsF_6)_2{\cdot}SO_2$ on the basis of elemental chemical analyses and the formation of large crystals. The tetragonal phase may be either a minor product, a salt of a new selenium–iodine cation, or another crystalline form of $Se_2I_4(AsF_6)_2$. Possibly it is a thermodynamically more stable phase that does not contain the SO_2 of crystallization.

Nature of $Se_2I_4(AsF_6)_2$ and $Se_2I_4(Sb_2F_{11})_2$ Solutions. The low-temperature ^{77}Se NMR spectra (−70 to −80 °C) obtained from $Se_2I_4(AsF_6)_2$ prepared in situ and by redissolving $Se_2I_4(AsF_6)_2$ and $Se_2I_4(Sb_2F_{11})$ in SO_2 were similar. They all showed the presence of SeI_3^+, Se_4^{2+}, and an unidentified peak at 1345 ppm having a peak width of ca. 6 Hz. Solid $Se_4(AsF_6)_2$, which was identified by Raman spectroscopy,[21] was precipitated from the $Se_2I_4(AsF_6)_2$ solution by cooling to −10 °C or lower. In addition, a single crystal of SeI_3AsF_6 was isolated from the supernatant solution after $Se_4(AsF_6)_2$ had been isolated and removed. The ^{77}Se NMR spectrum (−70 °C) of a solution of $Se_2I_4(AsF_6)_2$ and I_2 in a 1:1 mole ratio in SO_2 gave only one peak at 834 ppm (SeI_3^+). The reaction can therefore be described by eq 4. Thus,

$$Se_2I_4(AsF_6)_2 + I_2 \rightarrow 2SeI_3AsF_6 \qquad (4)$$

the presence of $Se_4(AsF_6)_2$ and SeI_3AsF_6 in $Se_2I_4(AsF_6)_2$ solution at low temperature is intrinsic and real. However, removal of the solvent at room temperature led to the formation of $Se_2I_4(AsF_6)_2$ with small amounts of a tetragonal phase as a possible minor product in some reactions.

The presence of SeI_3^+, Se_4^{2+}, and the unidentified species at 1345 ppm suggested $Se_2I_4^{2+}$ was likely involved in one or more equilibria. Attempts to correlate the relative integrated areas of the three peaks at various temperatures (with or without excess AsF_5) with various proposed equilibria (e.g. $Se_2I_4^{2+} \rightleftharpoons SeI_3^+ + {}^1/_4Se_4^{2+} + {}^1/_2I_2^+$) were not successful. The sharpness of the 1345 ppm peak (~6 Hz) indicates that it arises from a diamagnetic species. It can consistently be assigned to $Se_2I_4^{2+}$, but we cannot

---

(29) Frlec, B.; Holloway, J. H. *J. Chem. Soc., Dalton Trans.* **1975**, 535.

(30) Lau, C.; Passmore, J. *J. Chem. Soc., Dalton Trans.* **1973**, 2528.

(31) The ^{77}Se and ^{19}F NMR spectra of a solution of $Se_2I_4(AsF_6)_2$ in the presence of a large excess of AsF_5 (ca. 200% with respect to eq 2) showed that, after 30 days, SeI_3^+, $SeFI_2^+$, SeF_2I^+, and SeF_3^+ were formed. Presumably, $SeFI_2^+$, SeF_2I^+, and SeF_3^+ are products of a slow halogen-exchange reaction between the excess AsF_5 and SeI_3^+, one of the equilibrium products of $Se_2I_4(AsF_6)_2$, and/or $Se_2I_4^{2+}$ has slowly been oxidized by AsF_5 to $SeFI_2^+$, which then undergoes ligand exchange: Murchie, M. P.; Passmore, J. Unpublished results.

(32) Nakamoto, K. *Infrared Spectra of Inorganic and Co-ordination Compounds*, 2nd ed.; Wiley-Interscience: New York, 1970.

(33) Burns, R. C.; Gillespie, R. J.; Luk, W. C.; Slim, D. R. *Inorg. Chem.* **1979**, *18*, 3087.

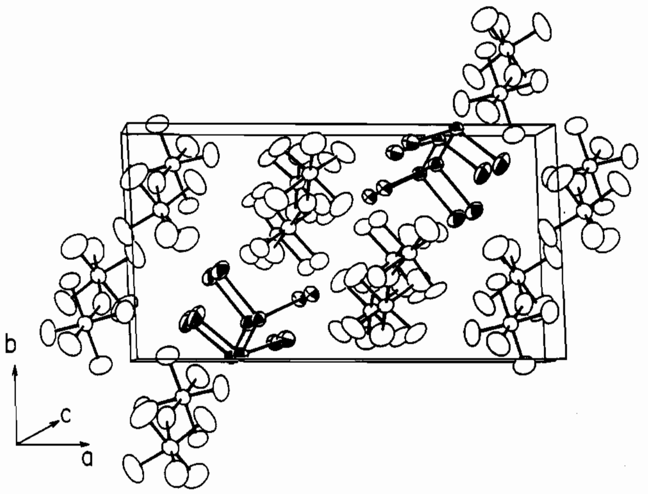

Figure 1. Crystal packing of $Se_2I_4(Sb_2F_{11})_2$.

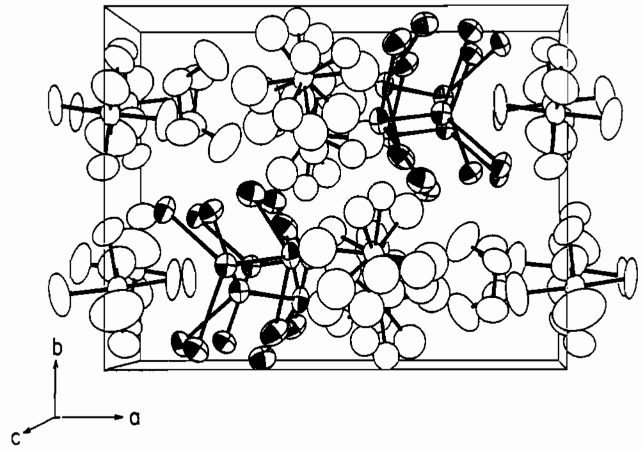

Figure 2. Crystal packing of $Se_2I_4(AsF_6)_2\cdot SO_2$.

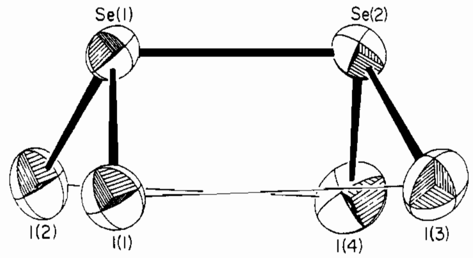

Figure 3. The $Se_2I_4^{2+}$ cation in $Se_2I_4(AsF_6)_2\cdot SO_2$.

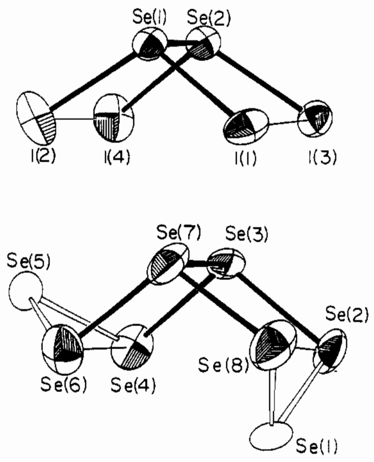

Figure 4. Structure of the $Se_2I_4^{2+}$ cation in $Se_2I_4(Sb_2F_{11})_2$ and the corresponding Se_6 atoms in the Se_8^{2+} cation in $Se_8(AlCl_4)_2$, in which the two Se_3^+ fragments are represented by shaded thermal ellipsoids

rule out that it might correspond to a new selenium–iodine cation or a new homopolyatomic selenium cation. The problem warrants further solution studies by a wide variety of techniques.

The $S_2O_4^{2-}$ anion, which is isovalent with the $Se_2I_4^{2+}$ cation, dissociates in solution to $SO_2^{\bullet-}$ radical anions according to eq 5.[34,35]

$$S_2O_4^{2-} \rightleftharpoons 2SO_2^{\bullet-} \qquad (5)$$

$$Se_2I_4^{2+} \rightleftharpoons 2SeI_2^{\bullet+} \qquad (6)$$

Preliminary magnetic susceptibility measurement of $Se_2I_4(AsF_6)_2$ in SO_2 solution at room temperature showed that it is diamagnetic within experimental uncertainty or, at the most, only very weakly paramagnetic. Thus, if $Se_2I_4^{2+}$ does dissociate to $SeI_2^{\bullet+}$ (e.g. eq 6), the equilibrium greatly favors $Se_2I_4^{2+}$ formation at room temperature.

X-ray Crystal Structure of $Se_2I_4(Sb_2F_{11})_2$ and $Se_2I_4(AsF_6)_2\cdot SO_2$. The crystal structures of $Se_2I_4(AsF_6)_2\cdot SO_2$ and $Se_2I_4(Sb_2F_{11})_2$ consist of columns of $Se_2I_4^{2+}$, AsF_6^-, and SO_2[36] and of $Se_2I_4^{2+}$ and $Sb_2F_{11}^-$, respectively (Figures 1 and 2) joined by weak cation–anion and cation–oxygen interactions. The $Se_2I_4^{2+}$ cation in the AsF_6^- salt is illustrated in Figure 3, and that in $Se_2I_4(Sb_2F_{11})_2$ is included in Figure 4. Appropriate bond distances and angles are presented in Tables V and VI.

Structure and Configuration of the $Se_2I_4^{2+}$ Cations. Both $Se_2I_4^{2+}$ cations have very similar eclipsed geometries of slightly distorted C_{2v} symmetry and are compared in Table VII. This suggests that the eclipsed structure of $Se_2I_4^{2+}$ is intrinsic and not a result of solid-state effects. The selenium–selenium bond distances in both $Se_2I_4(Sb_2F_{11})_2$ [2.841 (2) Å] and $Se_2I_4(AsF_6)_2\cdot SO_2$ [2.840 (6) Å] are essentially identical and very much longer than the selenium–selenium bond in α-Se_8 [2.336 (6) Å][38] but similar in length to the transannular bond in Se_8^{2+} [2.84 (1) Å][39] and the shorter selenium–selenium bond in Se_4N_4 [2.748 (9) Å].[40] The four selenium–iodine bonds in $Se_2I_4^{2+}$ are not equivalent in both salts [2.450 (2), 2.436 (2), 2.457 (2), and 2.443 (2) Å in $Se_2I_4(Sb_2F_{11})_2$; 2.446 (4), 2.457 (5), 2.460 (4), and 2.455 (5) Å in $Se_2I_4(AsF_6)_2\cdot SO_2$]. However, the average selenium–iodine bond distances in both $Se_2I_4(Sb_2F_{11})_2$ and $Se_2I_4(AsF_6)_2$ are similar [2.447 (2) and 2.455 (5) Å, respectively] and are shorter than those in SeI_3MF_6 [M = As, Sb; average Se–I = 2.510 (2) Å][4] and RSe–I

---

(34) Lough, L.; McDonald, J. W. *Inorg. Chem.* **1987**, *26*, 2024.

(35) Burlamacchi, L.; Casini, G.; Fagioli, O.; Tiezzi, E. *Ric. Sci.* **1967**, *37*, 97.

(36) It appears that the stacked column arrangement of the SO_2 molecules provides a low-energy pathway for loss of SO_2 in $Se_2I_4(AsF_6)_2\cdot SO_2$. However, a similar arrangement has also been observed in the crystal packing of $Se_6I_2(AsF_6)_2\cdot 2SO_2$,[6] and in this salt the SO_2 is not very labile. In addition, the SO_2 molecules in $Te_6(AsF_6)_4\cdot 2SO_2$,[33] which does not have the stacked column arrangement, are labile. Thus, the labile nature of SO_2 in $Se_2I_4(AsF_6)_2\cdot SO_2$ is not only a result of the stacked column arrangement. A comparison of the bond distances (i.e. strengths) of the contacts between SO_2 and the cations/anions with the sums of their corresponding isotropic van der Waals radii[42] in $Se_2I_4(AsF_6)_2\cdot SO_2$, $Se_6I_2(AsF_6)_2\cdot 2SO_2$, and $Te_6(AsF_6)_4\cdot 2SO_2$ indicated that they are similar in all salts. Presumably, a comparison of the lengths of the contacts in these salts with their corresponding sums of anisotropic van der Waals radii[37] might give a better assessment of the strength of these contacts. It may also be possible that the labile nature of SO_2 in these salts is a result of the weak electrostatic forces, e.g. dipole–dipole interactions.

(37) Nyburg, S. C.; Faerman, C. H. *Acta Crystallogr.* **1985**, *B41*, 274.

(38) Cherin, P.; Unger, P. *Acta Crystallogr.* **1972**, *B28*, 313.

(39) (a) McMullan, R. K.; Prince, D. J.; Corbett, J. D. *Inorg. Chem.* **1971**, *10*, 1749. (b) $Se_8(AsF_6)_2\cdot{}^1/_3SO_2$ had been prepared (ref 6, Experimental Section) and characterized by single-crystal X-ray diffraction analyses. Cell parameters: a = 29.5486 (12) Å, b = 8.753 (3) Å, c = 44.153 (13) Å, β = 106.52 (3)°, space group $C2/c$, Z = 24. The crystal contains three crystallographically different Se_8^{2+} ions, and they all have the exo–endo structure with bond distances and angles similar to those in $Se_8(AlCl_4)_2$ in ref 39a: Passmore, J.; Johnson, J. P.; Wong, C-M. Unpublished results.

(40) von Bärnighausen, H.; von Volkmann, T.; Jander, J. *Acta Crystallogr.* **1966**, *21*, 571.

(41) du Mont, W.-W.; Kubiniok, S.; Peters, K.; von Schnering, H.-G. *Angew. Chem., Int. Ed. Engl.* **1987**, *26*, 780.

Table V. Bond Distances (Å) for $Se_2I_4(Sb_2F_{11})_2$ and $Se_2I_4(AsF_6)_2{\cdot}SO_2$ (Esd's in Parentheses)

$Se_2I_4(Sb_2F_{11})_2$		$Se_2I_4(AsF_6)_2{\cdot}SO_2$	
Cation Contacts			
Se(1)–Se(2)	2.841 (2)	Se(1)–Se(2)	2.840 (6)
Se(1)–I(1)	2.450 (2)	Se(1)–I(1)	2.446 (4)
–I(2)	2.436 (2)	–I(2)	2.457 (5)
Se(2)–I(3)	2.457 (2)	Se(2)–I(3)	2.460 (4)
–I(4)	2.443 (2)	–I(4)	2.455 (5)
Anion Contacts			
Sb(1)–F(1)	1.88 (1)	As(1)–F(11)	1.63 (2)
–F(2)	1.84 (1)	–F(12)	1.67 (2)
–F(3)	1.83 (1)	–F(13)	1.69 (2)
–F(4)	1.86 (1)	–F(14)	1.71 (2)
–F(5)	1.84 (1)	–F(15)	1.73 (2)
–F(6)	2.00 (1)	–F(16)	1.68 (2)
Sb(2)–F(6)	2.05 (1)	As(2)[a]–F(21)	1.73 (4)
–F(7)	1.84 (1)	–F(22)	1.67 (5)
–F(8)	1.82 (1)	–F(23)	1.68 (6)
–F(9)	1.81 (1)	–F(24)	1.66 (4)
Sb(2)–F(10)	1.84 (1)	As(2)[a]–F(25)	1.73 (5)
–F(11)	1.85 (1)	–F(26)	1.66 (6)
Sb(3)–F(21)	1.83 (1)	As(2)[a]–F(31)	1.74 (4)
–F(22)	1.83 (1)	–F(32)	1.68 (5)
–F(23)	1.83 (1)	–F(33)	1.61 (6)
–F(24)	1.83 (1)	–F(34)	1.74 (4)
–F(25)	1.85 (1)	–F(35)	1.68 (5)
–F(26)	1.98 (1)	–F(36)	1.77 (4)
Sb(4)–F(26)	2.04 (1)	S–O(1)	1.42 (3)
–F(27)	1.86 (1)	–O(2)	1.39 (3)
–F(27)	1.86 (1)		
–F(28)	1.85 (1)		
–F(29)	1.82 (1)		
–F(30)	1.85 (1)		
–F(31)	1.85 (1)		
Intraionic Contacts[b]			
I(1)–I(3)	3.756 (2)	I(1)–I(3)	3.633 (4)
I(2)–I(4)	3.661 (2)	I(2)–I(4)	3.641 (4)
I(1)–I(2)	3.926 (2)	I(1)–I(2)	3.878 (4)
I(3)–I(4)	3.899 (2)	I(3)–I(4)	3.862 (4)
Interionic Contacts[b]			
Se(1)–F(1)	2.84 (1)	Se(1)–F(21)	2.91 (4)
–F(8)	2.92 (1)	–F(23)	2.86 (5)
–F(23)	2.91 (1)	–F(31)	3.26 (4)
–F(29)	3.24 (1)	–F(33)	3.32 (5)
		–F(35)	3.13 (5)
Se(2)–F(1)	2.99 (1)	Se(2)–F(21)	2.89 (4)
–F(23)	2.92 (1)	–F(22)	3.22 (5)
		–F(24)	3.19 (4)
		–F(31)	2.99 (4)
		–F(34)	2.94 (4)
		–F(36)	3.23 (4)
I(1)–F(21)	3.33 (1)	I(1)–F(15)	2.83 (2)
–F(24)	3.00 (1)	–F(15′)	3.43 (2)
–F(27)	3.31 (1)	–F(16)	3.46 (2)
–F(29)	3.49 (1)		
I(2)–F(2)	3.08 (1)	I(2)–F(14)	3.02 (3)
–F(5)	3.39 (1)	–F(16)	3.47 (2)
–F(7)	3.49 (1)		
–F(11)	3.44 (2)		
I(3)–F(25)	3.31 (1)	I(3)–O(2)	2.97 (2)
I(3)–F(28)	2.89 (1)	I(3)–F(12)	3.37 (3)
		–F(34)	3.37 (4)
		–F(36)	3.19 (5)
I(4)–F(3)	2.96 (1)	I(4)–O(1)	3.11 (3)
–F(9)	3.35 (2)	–F(12)	3.47 (2)
–F(10)	3.35 (2)	–F(24)	3.11 (5)
		–F(33)	3.25 (6)
		–F(35)	3.21 (5)
		–I(4′)	4.145 (5)[c]
		S–F(11)	3.14 (4)
		–F(13)	3.10 (2)
		–F(16)	3.15 (2)

[a] The AsF_6^- anion is disordered and is modeled by refining two cocentric AsF_6^- anions with 50% occupancy each. [b] Includes all contacts less than the sum of the van der Waals radii (Se–Se = 4.00, Se–I = 4.15, I–O = 4.30, Se–F = 3.35, Se–O = 3.50, I–F = 3.50, I–O = 3.65 Å).[42] [c] Cation–cation contact.

Table VI. Bond Angles (deg) for $Se_2I_4(Sb_2F_{11})_2$ and $Se_2I_4(AsF_6)_2{\cdot}SO_2$ (Esd's in Parentheses)

$Se_2I_4(Sb_2F_{11})_2$		$Se_2I_4(AsF_6)_2{\cdot}SO_2$	
Cation Contacts			
I(1)–Se(1)–I(2)	106.95 (8)	I(1)–Se(1)–I(2)	104.5 (2)
I(3)–Se(2)–I(4)	105.47 (8)	I(3)–Se(2)–I(4)	103.6 (1)
Se(1)–Se(2)–I(3)	101.03 (7)	Se(1)–Se(2)–I(3)	99.2 (2)
–I(4)	101.26 (7)	–I(4)	98.3 (2)
Se(2)–Se(1)–I(1)	100.47 (7)	Se(2)–Se(1)–I(1)	99.3 (2)
–I(2)	98.07 (7)	–I(2)	100.3 (2)
		O(1)–S–O(2)	114 (2)
Intraionic Contacts[a]			
Se(1)–I(1)–I(3)	79.55 (5)	Se(1)–I(1)–I(3)	80.8 (1)
Se(1)–I(2)–I(4)	81.65 (6)	Se(1)–I(2)–I(4)	79.7 (1)
Se(2)–I(3)–I(1)	78.93 (5)	Se(2)–I(3)–I(1)	80.5 (1)
Se(2)–I(4)–I(2)	78.96 (5)	Se(2)–I(4)–I(2)	81.4 (1)
Interionic Contacts[a]			
I(1)–Se(1)–F(1)	158.8 (3)	I(1)–Se(1)–F(21)	86.0 (8)
–F(8)	122.6 (3)	–F(23)	167.4 (11)
–F(23)	83.9 (3)	–F(31)	157.4 (8)
–F(29)	74.3 (2)	–F(35)	79.9 (8)
I(2)–Se(1)–F(1)	89.8 (3)	I(2)–Se(1)–F(21)	159.6 (9)
–F(8)	95.3 (3)	–F(23)	88.0 (11)
F(23)	158.4 (2)	–F(31)	79.9 (8)
–F(29)	138.5 (3)	–F(35)	167.9 (9)
I(3)–Se(2)–F(1)	154.2 (3)	I(3)–Se(2)–F(21)	82.7 (7)
–F(23)	82.9 (3)	–F(22)	132.4 (9)
		–F(24)	166.4 (9)
		–F(31)	167.1 (9)
		–F(34)	76.6 (8)
		–F(36)	138.7 (8)
I(4)–Se(2)–F(1)	94.3 (3)	I(4)–Se(2)–F(21)	159.3 (9)
–F(23)	161.6 (3)	–F(22)	123.8 (9)
		–F(24)	82.8 (8)
		–F(31)	80.4 (8)
		–F(34)	179.0 (9)
		–F(36)	111.5 (8)
Se(1)–I(1)–F(21)	124.2 (3)	Se(1)–I(1)–F(15)	176.7 (5)
–F(24	163.4 (3)	–F(15)′	123.3 (4)
–F(27)	122.8 (2)	–F(16)	91.8 (4)
–F(29)	63.2 (2)		
Se(1)–I(2)–F(2)	147.9 (2)	Se(1)–I(2)–F(14)	173.3 (5)
–F(5)	103.6 (2)	–F(16)	131.3 (4)
–F(7)	119.9 (3)		
–F(11)	141.2 (2)		
Se(2)–I(3)–F(25)	123.6 (3)	Se(2)–I(3)–O(2)	165.3 (6)
–F(28)	169.5 (3)	–F(12)	89.2 (5)
		–F(34)	58.1 (7)
		–F(36)	131.5 (8)
Se(2)–I(4)–F(3)	159.0 (2)	Se(2)–I(4)–O(1)	149.4 (6)
–F(9)	121.5 (3)	–F(12)	87.1 (5)
–F(10)	144.5 (3)	–F(24)	148.9 (9)
		–F(33)	85.9 (10)
		–F(35)	147.5 (9)
		–I(4′)	98.8 (1)[b]

[a] Includes all contacts less than the sum of the van der Waals radii (Se–Se = 4.00, Se–I = 4.15, Se–F = 3.35, Se–O = 3.50, I–F = 3.65, I–O = 3.55 Å).[42] [b] Cation–cation contact.

[R = 2,4,6-*t*-$Bu_3(C_6H_2)$; Se–I = 2.529 Å][41] but similar to that in $Se_6I_2(AsF_6)_2{\cdot}SO_2$ [2.454 (2) Å].[6]

The average torsional angles defined by I(1)–Se(1)–Se(2)–I(3) and I(2)–Se(1)–Se(2)–I(4) in $Se_2I_4(Sb_2F_{11})_2$ and $Se_2I_4(AsF_6)_2{\cdot}SO_2$ (2.0 and 4.2°, respectively) are close to 0°. Thus, the syn iodine atoms [I(1)–I(3) and I(2)–I(4)] are essentially eclipsed and the $Se_2I_4^{2+}$ cations in both salts can be considered as having idealized C_{2v} symmetry. The overall configuration of the eclipsed $Se_2I_4^{2+}$ cation resembles a distorted trigonal prism. There are significant intracationic interactions between the syn iodine atoms [average 3.709 (2) and 3.637 (4) Å in $Se_2I_4(Sb_2F_{11})_2$ and $Se_2I_4(AsF_6)_2{\cdot}SO_2$, respectively]. These interactions are significantly less than twice the sum of van der Waals radii of iodine (4.30 Å)[42] but longer

---

(42) Pauling, L. *The Nature of Chemical Bond*, 3rd ed.; Cornell University Press: Ithaca, NY, 1960.

Table VII. Comparison of the Geometries of the $Se_2I_4^{2+}$, $S_2I_4^{2+}$, $S_2O_4^{2-}$, S_8^{2+}, and Se_8^{2+} Ions

	$Se_2I_4^{2+}$ [a]				
	$Se_2I_4(Sb_2F_{11})_2$	$Se_2I_4(AsF_6)_2{\cdot}SO_2$	$S_2I_4^{2+}$ [b]	$S_2O_4^{2-}$ [c]	Se_8^{2+} [d]
		Average Bond Distances (Å)[e]			
$M-M_o$	2.841 (2)	2.840 (6)	1.817 (10)	2.386 (2)	2.84 (1)
$M-X_o$	2.447 (2)	2.455 (5)	2.993 (4)	1.514 (3)	2.33 (1)
$X-X_o$	3.709 (2)	3.637 (4)	2.571 (2)	2.742 (4)	3.32 (1)
		Average Bond Angles (deg)[e]			
$X-M-X'$	106.2 (1)	104.1 (2)	90.4 (2)	110.4 (2)	101.3 (5)
$M-M_o-X_o$	100.2 (1)	99.3 (2)	97.2 (2)	97.8 (2)	95.8 (4)
		Average Torsional Angles (deg)[e]			
$X-M-M_o-X_o$	2.0	4.2	0	0	2.5
		Dihedral Angles (deg)[e]			
$XMX'-X_oM_oX_o'$	34.4	30.4	20.6	23.8	18.3
$XMM_oX_o-X'MM_oX_o'$	108.7	105.9	90.1	111.5	101.9

[a] This work. [b] From the symmetric $S_2I_4^{2+}$ cation in $S_2I_4(SbF_6)_2$.[3] [c] From the $S_2O_4^{2-}$ anion in $ZnS_2O_4{\cdot}C_5H_5N$.[16] [d] From the Se_8^{2+} cation in $Se_8(AlCl_4)_2$.[39] [e] The configuration studied is

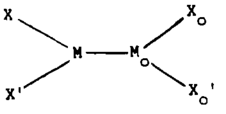

where M = Se and X = I for $Se_2I_4^{2+}$, M = S and X = I for $S_2I_4^{2+}$, M = S and X = O for $S_2O_4^{2-}$, and M = Se(3), Se(7) and X = Se(2), Se(4), Se(6), Se(8) for Se_8^{2+}.

than the iodine–iodine intraionic contacts between the I_2^+ cations in I_4^{2+} [3.264 (7) Å][43] and the I_5^+ cations in I_{15}^{3+} [3.416 (3) Å].[44] The intraionic iodine–iodine interactions are likely of a bonding nature or the cation would not be exactly eclipsed or would have adopted the structure of the less sterically hindered isomer, σ-bonded *trans*-$Se_2I_4^{2+}$ (**1c**), similar to that of P_2I_4.[14]

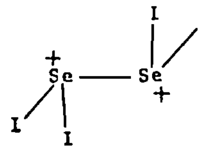

1c

Bonding in the $Se_2I_4^{2+}$ Cation. The bonding in $Se_2I_4^{2+}$ may be described by valence-bond structure **2**, with lesser contributions from structures **3** and **4**.

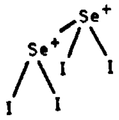

2

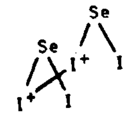

3

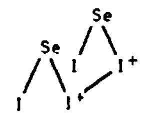

4

This model is consistent with the long selenium–selenium bond [average 2.841 (6) Å; bond order ca. 0.2[45]], the significant intraionic iodine–iodine interactions in both $Se_2I_4(Sb_2F_{11})_2$ and $Se_2I_4(AsF_6)_2{\cdot}SO_2$ [average 3.709 (2) and 3.637 (4) Å, respectively], and the appreciable cation–anion interactions between the iodine atoms and the anionic fluorine atoms in both salts. $Se_2I_4^{2+}$ is clearly not a simple iodo derivative of the 1,5-diselenacyclooctane dication (**1a**),[17d] represented by structure **2**, as the sulfur–sulfur bond length in the sulfur[17e] analogue (**1b**) is 2.1243 (Å) (average); i.e., it contains a normal S–S bond with some lengthening due to electrostatic repulsion.

Alternatively, the $Se_2I_4^{2+}$ cation may be regarded as two $SeI_2^{\bullet+}$ radical cations joined by the overlap of the odd electron in each π* SeI_2^+ SOMO (singly occupied molecular orbital), as shown in Figure 5. This results in some bonding between all six atoms and a formal selenium–iodine bond order of 1.25 (net 0.5 π bond per $SeI_2^{\bullet+}$ unit). This is consistent with the fact that the average Se–I bond distances in $Se_2I_4(Sb_2F_{11})_2$ and $Se_2I_4(AsF_6)_2{\cdot}SO_2$ [2.447 (2) and 2.455 (5) Å, respectively] are shorter than the formal single bond in SeI_3MF_6 [M = As, Sb; average Se–I = 2.510 (2) Å][4] and 2,4,6-*t*-$Bu_3C_6H_2Se$–I (2.529 Å).[41] Thus, the structural feature of $Se_2I_4^{2+}$ can be explained in terms of a 6-center, 2-electron π*–π* bond involving the interaction of π* SOMO's of each $SeI_2^{\bullet+}$, as illustrated in Figure 5.

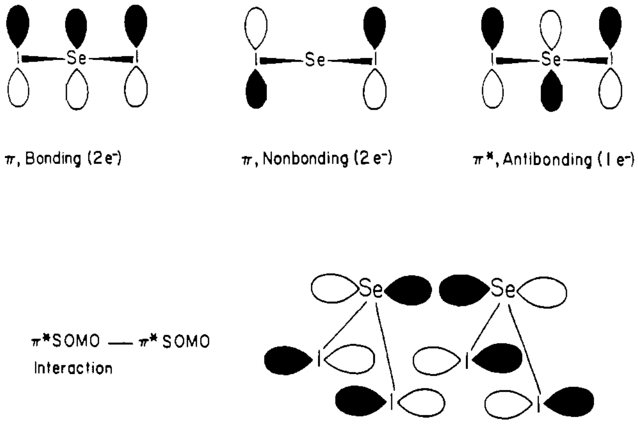

Figure 5. $SeI_2^{\bullet+}$ radical cation π MO's derived from p_y selenium and iodine AO's and the π* SOMO–π* SOMO interaction in $Se_2I_4^{2+}$.

In order to test the proposed π*–π* bonding model, the $S_2Cl_4^{2+}$ cation[46] was chosen as a model for $Se_2I_4^{2+}$ and its electronic structure was calculated by using the ab initio STO-3G method (nonoptimized). All the molecular orbitals that exhibit interaction between the two $SCl_2^{\bullet+}$ moieties having a bonding and an antibonding MO counterpart, both of which are occupied, and these are shown in Figure 6 [e.g., MO 42 (bonding) and MO 47 (antibonding)], except for MO 49 which is the HOMO. Therefore, MO 49 is responsible for the bonding between the two $SCl_2^{\bullet+}$ radical cations and can be viewed as a π* SOMO–π* SOMO interaction, consistent with that illustrated in Figure 5 for $Se_2I_4^{2+}$. The antibonding counterpart of MO 49 is the LUMO (MO 50). In addition, MO's 37 and 43 are π bonding with respect to the

---

(43) Gillespie, R. J.; Kapoor, R.; Faggiani, R.; Lock, C. J. L.; Muchie, M. P.; Passmore, J. *J. Chem. Soc., Chem. Commun.* **1983**, 8.

(44) Passmore, J.; Taylor, P.; Whidden, T.; White, P. S. *Can. J. Chem.* **1979**, *57*, 968.

(45) Selenium–selenium bond order: $n = 10^{(2.35-R)}/0.71$, where *R* is the Se–Se bond distance (Å); from ref 42.

(46) The $S_2Cl_4^{2+}$ cation has C_{2v} symmetry: S–S = 2.39, S–Cl = 1.94 Å; S–S–Cl = 100, Cl–S–Cl = 104°.

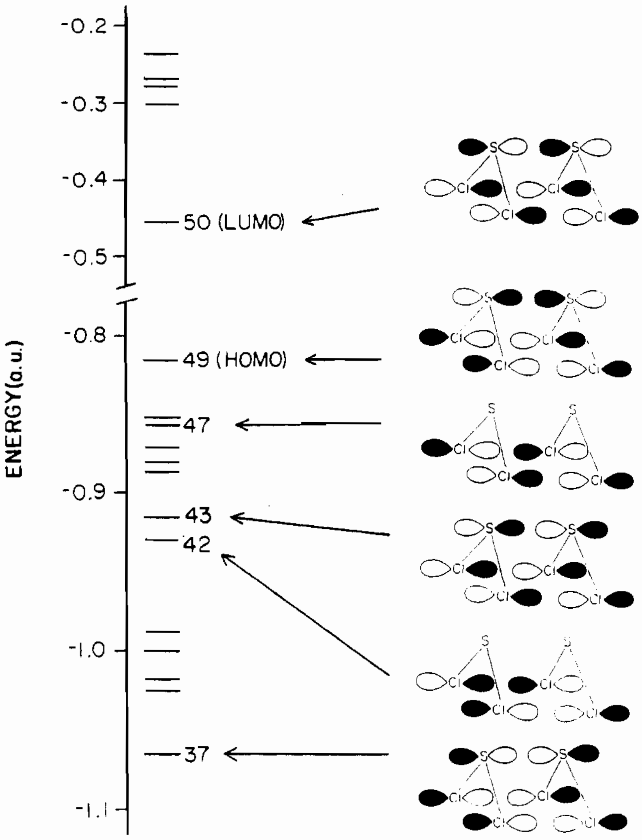

Figure 6. Molecular orbitals of $S_2Cl_4^{2+}$: a model for the $Se_2I_4^{2+}$ cation.

S–Cl bond, whereas MO 42 and MO 47 are nonbonding, and MO 49 is antibonding (Figure 6). Thus, to the first order of approximation, one π bond is distributed over all six atoms, giving a formal S–Cl bond order of 1.25 (net: one π bond per $S_2Cl_4^{2+}$ or per four S–Cl bonds). This is consistent with the simple MO model for $SeI_2^{\bullet+}$ and $Se_2I_4^{2+}$ (Figure 5), in which there is 4pπ–5pπ bonding between the selenium and iodine atoms with a formal bond order of 1.25. This represents an example of an exception to the "double-bond rule",[47] that is, the thermodynamic preference for homoatomic σ bonds over *n*pπ–*n*pπ bonds for heavier main-group elements ($n > 3$). This reflects the observation that neutral compounds of silicon, phosphorus, or sulfur containing *n*pπ–*n*pπ bonds are unstable with respect to oligomerization. Exceptions to the rule have been provided by means of kinetic stabilization [e.g. $(Me_3Si)_3CP{=}PC(SiMe_3)_3$].[48] However, thermodynamically stable *n*pπ–*n*pπ ($n > 3$) bonds have been observed in many of the homoatomic cations[17b] (e.g. S_4^{2+},[49] I_4^{2+}[43]) and chalcogen–halogen cations related to $Se_2I_4^{2+}$[17a] (e.g. $S_2I_4^{2+}$,[3] $Br_2Se^+SeSeBr$,[50] $Se_6I_2^{2+}$[6]) as well as in various neutral and ionic sulfur species (e.g. S_2F_2,[51a] S_2^- in solution[51b]).

The $Se_2I_4^{2+}$ Cation and the Isovalent Species. The $Se_2I_4^{2+}$ cation is isovalent[52] with neutral As_2I_4 and P_2I_4 (**5**),[14] the $S_2I_4^{2+}$ cation in $S_2I_4(MF_6)_2$ (M = As, Sb)[3] (**6**), and the $S_2O_4^{2-}$ anion in $Na_2S_2O_4$[15] and $ZnS_2O_4{\cdot}C_6H_5N$[16] (**7**).

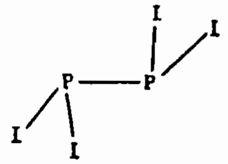

5

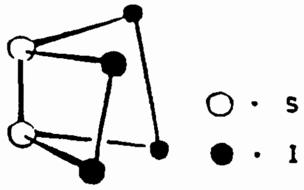

6

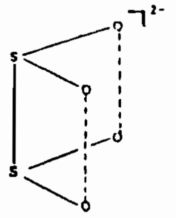

7

Neutral P_2I_4 adopts the trans configuration **5** with a normal 2-center, 2-electron phosphorus–phosphorus bond [2.21 (6) Å; cf. 2.21 (2) Å in P_4].[53,54] Presumably, the trans configuration of P_2I_4 (**5**) minimizes repulsion between the lone pairs. In this structure there is no contribution from valence-bond structure **8**

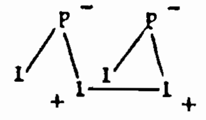

8

(cf. valence-bond structures **3** and **4** for $Se_2I_4^{2+}$). This is because autoionization with resulting charge localization onto the iodine atoms, as shown in structure **8**, is energetically unfavorable. [Note: Iodine is more electronegative ($\chi_I = 2.5$) than phosphorus ($\chi_P = 2.1$).] In contrast, the equivalent valence-bond structures for $Se_2I_4^{2+}$ (**3** and **4**) allow for some positive charge delocalization and therefore lower the energy of the system. Positive charge delocalization is an important feature in cations of this class and is one factor in achieving cluster formation and *n*pπ–*n*pπ bonding ($n \geq 3$).[17a,b] Thus, charge delocalization, Se–I π bonding, and the π*–π* interaction favor the cluster-like structure for $Se_2I_4^{2+}$ rather than that of the σ-bonded *trans*-$Se_2I_4^{2+}$ isomer (**1c**). The bond energy of the adjacent Se^+–Se^+ σ bond in **1c** (46 kcal mol^{-1} in neutral -Se–Se-)[55] is therefore less than the sum of the delocalized selenium–iodide 4pπ–5pπ bond, the π*–π* bond, and the positive charge delocalization energy in $Se_2I_4^{2+}$.

The structure of the $S_2I_4^{2+}$ cation, the sulfur analogue of $Se_2I_4^{2+}$, in $S_2I_4(MF_6)_2$ (M = As, Sb)[3] approximates that of a distorted right triangular prism (**6**) but is very different in geometry from $Se_2I_4^{2+}$ (see Introduction and Table VII). The $S_2I_4^{2+}$ cation may be regarded[3] as consisting of $S_2^{0.66+}$ and two $I_2^{0.66+}$ units, weakly bonded together by electrons in mutually perpendicular π* orbitals (**9**).

The fact that the $Se_2I_4^{2+}$ structure is different from that of $S_2I_4^{2+}$ supports our hypothesis[3] that the unique $S_2I_4^{2+}$ structure arises from the near equality of the ionization energies of S_2 [9.36 (2) eV] and I_2 (9.3995 (12) eV].[13] [N.B. The IE of Se_2 [8.88 (3) eV][13] is substantially lower than that of I_2.] However, both contain *n*pπ–*n*pπ and π*–π* bonds and have cluster-like characteristics.

---

(47) (a) Cowley, A. H. *Acc. Chem. Res.* **1984**, *17*, 386. (b) Schmidt, M. W.; Truong, P. N.; Gordon, M. S. *J. Am. Chem. Soc.* **1987**, *109*, 5217.

(48) Cowley, A. H.; Kilduff, J. E.; Lasch, J. G.; Mehrotra, S. K.; Norman, N. C.; Pakulski, M.; Wittlesey, B. R.; Atwood, J. L.; Hunter, W. E. *Inorg. Chem.* **1984**, *23*, 2582.

(49) Passmore, J.; Sutherland, G. W.; White, P. S. *J. Chem. Soc., Chem. Commun.* **1980**, 330.

(50) Passmore, J.; Tajik, M.; White, P. S. *J. Chem. Soc., Chem. Commun.* **1988**, 175.

(51) (a) Kuczkowski, R. L.; Wilson, E. B. *J. Am. Chem. Soc.* **1963**, *85*, 2028. Kuczkowski, R. L. *J. Am. Chem. Soc.* **1964**, *86*, 3617. (b) Chivers, T. In *Homoatomic Rings, Chains and Macro-molecules of the Main Group Elements*; Rheingold, A. L., Ed.; Elsevier: New York, 1977; p 499.

(52) These species are isovalent in the sense that they contain the same number of valence electrons.

(53) Steudel, R. In *Sulfur* (*Studies in Inorganic Chemistry*); Muller, A., Krebs, B., Eds.; Elsevier: New York, 1984; p 3.

(54) Maxwell, L. R.; Hendricks, S. B.; Mosley, V. M. *J. Chem. Phys.* **1935**, *3*, 699.

(55) Dasent, W. E. *Inorganic Energetics*, 2nd ed.; Cambridge University Press: Cambridge, England, 1982.

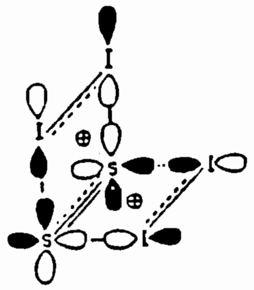

9

The structures of both cations may formally be derived from different isomers of benzene: $S_2I_4^{2+}$ (**11**) from Dewar benzene (**10**) and $Se_2I_4^{2+}$ (**13**) from prismane benzene (**12**). The configuration of $Se_2I_4^{2+}$ is related to that of M_6^{2+} (i.e. $Te_3S_3^{2+}$ and $Te_2Se_4^{2+}$)[56] and Te_6^{4+}.[33] In the context of Gillespie's model,[57] $Se_2I_4^{2+}$, M_6^{2+}, and Te_6^{4+} may all be regarded as being derived from the electron-precise trigonal-prismatic cluster **12** by adding four, two, and one electron pairs, respectively. This, though, gives a classical σ-bonded structure for $Se_2I_4^{2+}$, as is depicted in **13**. To obtain the observed structure, the intraionic $SeI_2^{\bullet+}$–$SeI_2^{\bullet+}$ π^*–π^* interaction must replace the full Se^+–Se^+ bond in structure **13**. However, within the context of the simple MO model we propose, the high symmetry of $Se_2I_4^{2+}$ arises from the presence of the intercationic π^*–π^* bond directly.

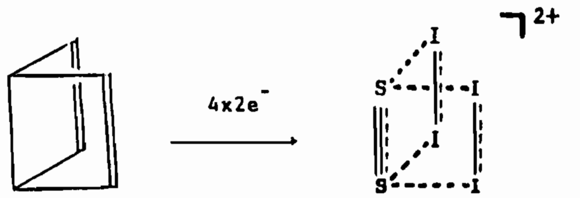

10

11

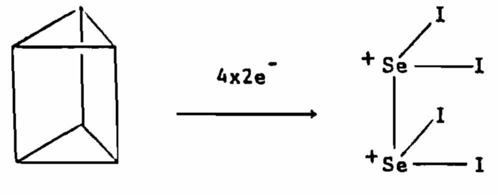

12

13

The eclipsed $S_2O_4^{2-}$ anions in both $Na_2S_2O_4$[15] and $ZnS_2O_4 \cdot C_5H_5N$[16] have distorted C_{2v} symmetries, and a comparison of geometries of the $Se_2I_4^{2+}$ and $S_2O_4^{2-}$ ions is presented in Table VII. The sulfur–oxygen bond in $S_2O_4^{2-}$ (1.51 Å) is somewhat shorter than a related single bond (single S–O bond distance estimated by using the Schoemaker–Stevenson equation, 1.69–1.70 Å),[58] while the sulfur–sulfur bond (2.39 Å) is much longer than the single bond in S_8 (2.05 Å).[53] Thus, the structural features of $Se_2I_4^{2+}$ and $S_2O_4^{2-}$ are very similar and the bonding in $S_2O_4^{2-}$ can be accounted for by a similar 6-center, 2-electron π^*–π^* bond between the π^* SOMO's of each of two $SO_2^{\bullet-}$ radical anions.

Structural Relationship between $Se_2I_4^{2+}$ and Se_8^{2+}. Implication for the Nature of the Bonding in Se_8^{2+} and S_8^{2+}. The structure of Se_8^{2+} in $Se_8(AlCl_4)_2$[39a] and in $Se_8(AsF_6)_2 \cdot {}^1/_3SO_2$[39b] has a puckered, eight-membered-ring conformation as shown in Figure 4. The two parallel –Se–Se⁺–Se– units [–Se(2)–Se(3)⁺–Se(4)– and –Se(6)–Se(7)–Se(8)–] (see Figure 4) are well within the sum of van der Waals radii of 4 Å for selenium [Se(2)–Se(8) = 3.35 (1), Se(3)–Se(7) = 2.84 (1), and Se(4)–Se(6) = 3.29 (1) Å]. The structure of Se_8^{2+} has been found to be rigid in solution from ^{77}Se NMR data, and there is coupling between the cross-ring selenium atoms [Se(2)–Se(8) = 25.6, Se(3)–Se(7) = 78.9, and Se(4)–Se(6) = 91.3 Hz].[59] Thus, it is likely the cross-ring interactions are real and correspond to some degree of bonding, and are not a result of solid-state effects.

The Se–Se bond distance in $Se_2I_4^{2+}$ [2.841 (4) Å] is identical with the transannular distance between the two formally positively charged selenium atoms [Se(3)–Se(7) = 2.84 (1) Å] in Se_8^{2+}. The configurations of the two parallel –Se–Se⁺–Se– units are similar to those of the two $SeI_2^{\bullet+}$ in the $Se_2I_4^{2+}$ cation and are illustrated in Figure 4. Thus, the long transannular selenium–selenium bond in Se_8^{2+} has been "isolated" in $Se_2I_4^{2+}$. A comparison of their bond angles, torsional angles, and dihedral angles is given in Table VII. The Se–Se bonds adjacent to the formally tricoordinate selenium atoms, Se(3) and Se(7), have an average distance 2.33 (1) Å, which, although not significantly shorter than that in α-Se_8 of 2.336 (6) Å, is not inconsistent with the presence of some $4p\pi$–$4p\pi$ bonding. They are certainly not long, as would be expected for chalcogen–chalcogen bonds adjacent to a positively charged tricoordinate chalcogen atom [e.g. average Se_{tri}–Se_{di} = 2.43 (1) Å in Se_{10}^{2+}].[60,61] Since the electronegativities of Se and I are similar and –Se– is isovalent with –I, the –Se–Se⁺–Se– units in Se_8^{2+} can be considered as isovalent with $SeI_2^{\bullet+}$. This strongly suggests that the bonding in $Se_2I_4^{2+}$ and the bridging portions of Se_8^{2+} (and S_8^{2+}) are very similar. This is supported by an extended Hückel molecular orbital study of S_8^{2+},[62a] which also has a puckered, eight-membered-ring structure[62b] very similar to that of Se_8^{2+}. All of the molecular orbitals exhibiting cross-ring characteristics have a bonding and an antibonding counterpart occupied except the HOMO-1, which can be viewed as a 6-center, 2-electron π^*–π^* interaction (**14**)[62a] and is similar to those illustrated for $Se_2I_4^{2+}$ and $S_2Cl_4^{2+}$ (MO 49) in Figures 5 and 6. Thus, the bonding situations in $Se_2I_4^{2+}$, Se_8^{2+}, and S_8^{2+} are similar in that they all contain an intracationic π^*–π^* bond.

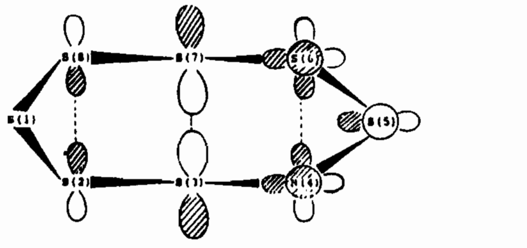

14

A variety of other stable main-group radicals dimerize via multicenter 2-electron π^*–π^* bonds.[17b] These include solid $(NO)_2$,[63] I_4^{2+} (4-center, 2-electron π^*–π^* bonds),[43] and solid N_2O_4 (planar).[64] In addition, a number of heterocyclic π^*-radical systems are dimeric in the solid state; e.g., $(S_3N_2^+)_2$,[65] $(C_6H_4S_2N)_2$,[66] and RCNSSN (e.g. R = CF_3)[67,68] are also bonded via

---

(56) Gillespie, R. J.; Luk, W. C.; Maharajh, E.; Slim, D. R. *Inorg. Chem.* **1977**, *16*, 892.

(57) Gillespie, R. J. *Chem. Soc. Rev.* **1979**, *8*, 315.

(58) Schoemaker, V.; Stevenson, D. P. *J. Am. Chem. Soc.* **1941**, *63*, 37.

(59) Burns, R. C.; Collins, M. J.; Gillespie, R. J.; Schrobilgen, G. J. *Inorg. Chem.* **1986**, *25*, 4465.

(60) Burns, R. C.; Chan, W. C.; Gillespie, R. J.; Luk, W. C.; Sawyer, J. F.; Slim, D. R. *Inorg. Chem.* **1980**, *19*, 1432.

(61) Collins, M. J.; Gillespie, R. J.; Sawyer, J. F.; Schrobilgen, G. J. *Acta Crystallogr.* **1986**, *C42*, 13.

(62) (a) Burford, N.; Passmore, J. Unpublished results. (b) Davies, C. G.; Gillespie, R. J.; Park, J. J.; Passmore, J. *Inorg. Chem.* **1971**, *10*, 2781.

(63) Lipscomb, W. N.; Wang, F. E.; May, W. R.; Lippert, E. L. *Acta Crystallogr.* **1961**, *14*, 1100.

(64) Groth, P. *Nature* **1963**, *198*, 1081.

(65) Gillespie, R. J.; Kent, J. P.; Sawyer, J. F. *Inorg. Chem.* **1981**, *20*, 3784 and references therein.

(66) (a) Awere, E. G.; Burford, N.; Mailer, C.; Passmore, J.; Schriver, M. J.; White, P. S.; Banister, A. J.; Oberhammer, H.; Sutcliffe, L. H. *J. Chem. Soc., Chem. Commun.* **1987**, 66. (b) Awere, E. G.; Burford, N.; Haddon, R. C.; Parsons, S.; Passmore, J.; Waszlzak, J. V.; White, P. S. *Inorg. Chem.*, in press.

(67) Höfs, H.-U.; Bats, J. W.; Gleiter, R.; Hartmann, G.; Mews, R.; Eckert-Maksie, M.; Oberhammer, H.; Sheldrick, G. M. *Chem. Ber.* **1985**, *118*, 3781.

(68) Cordes, A. W.; Goddard, J. D.; Oakley, R. T.; Westwood, N. P. C. *J. Am. Chem. Soc.* **1989**, *111*, 6147 and references therein.

overlap of the π^* SOMO's of the corresponding radical monomers.

Comparison of the $Se_2I_4^{2+}$ Bond Distances and Angles in $Se_2I_4(Sb_2F_{11})$ and $Se_2I_4(AsF_6)_2{\cdot}SO_2$. The bond distances and angles of the $Se_2I_4^{2+}$ cations in $Se_2I_4(Sb_2F_{11})_2$ and $Se_2I_4(AsF_6)_2{\cdot}SO_2$ are given in Tables V and VI. The selenium–selenium bond distances in both $Se_2I_4(Sb_2F_{11})_2$ [2.841 (2) Å] and $Se_2I_4(AsF_6)_2{\cdot}SO_2$ [2.840 (6) Å] are essentially identical. The four selenium–iodine bonds in both $Se_2I_4(Sb_2F_{11})_2$ and $Se_2I_4(AsF_6)_2{\cdot}SO_2$ are not equivalent, but they are all significantly shorter than the selenium–iodine distance in the SeI_3MF_6 (M = As, Sb).[4] The differences between the shortest and longest selenium–iodine bonds within each cation are 0.021 Å in $Se_2I_4(Sb_2F_{11})_2$ [Se(1)–I(2) = 2.436 (2) and Se(2)–I(3) = 2.457 (2) Å] and 0.014 Å in $Se_2I_4(AsF_6){\cdot}SO_2$ [Se(1)–I(1) = 2.446 (4) and Se(2)–I(3) = 2.460 (4) Å]. The differences are higher than twice the standard deviation of the bond distances and are significant. In both salts, the Se(1)–I(1) and Se(1)–I(2) bonds are shorter than the Se(2)–I(3) and Se(2)–I(4) bonds, respectively (Table Ve. Consistently, the I(1)–Se(1)–I(2) angles [106.95 (8) and 104.5 (2)°] are larger than the I(3)–Se(2)–I(4) angles [105.47 (8) and 103.6 (1)°] in both $Se_2I_4(Sb_2F_{11})_2$ and $Se_2I_4(AsF_6)_2{\cdot}SO_2$, respectively. This is in accord with the predictions of the VSEPR model that shorter adjacent bonds have larger bond angles.[69] However, no correlations between Se–Se–I bond angles and Se–I bond distances are observed. Attempts to correlate the interionic contacts (i.e. Se- - -F and I- - -F) and the variation of selenium–iodine bond lengths were inconclusive. It is likely tht the variation of the selenium–iodine bond distances arises from solid-state effects. Alternatively, in valence-bond terms, the structure of the cation may be described, in part, as comprising a SeI_2^{2+} dication [i.e. $I(1)Se(1)I(2)^{2+}$] and a neutral SeI_2 unit [i.e. I(3)Se(2)I(4)] with strong interaction between the dication and neutral SeI_2. This is consistent with the observation that the cation–anion contacts involving Se(1) in both $Se_2I_4(Sb_2F_{11})_2$ and $Se_2I_4(AsF_6)_2{\cdot}SO_2$ are shorter and more numerous than those involving Se(2) (Table V).

Cation–Anion Contacts. There are significant interionic interactions between the selenium and iodine atoms in $Se_2I_4^{2+}$ and the anionic fluorine atoms. In addition, the SO_2 in $Se_2I_4(AsF_6)_2{\cdot}SO_2$ also shows significant interactions with the $Se_2I_4^{2+}$ and AsF_6^- ions (Table V). This is consistent with significant charge delocalization over all atoms in the cation. A description (with figures) of the complete coordination around the selenium and iodine atoms is given in the supplementary material.

The $Sb_2F_{11}^-$ and AsF_6^- Anions and SO_2. The two crystallographically independent $Sb_2F_{11}^-$ anions in $Se_2I_4(Sb_2F_{11})_2$ contain bent asymmetric Sb–F–Sb bridge arrangements [Sb(1)–F(6) = 2.00 (1) Å, Sb(2)–F(6) = 2.05 (1) Å, Sb(1)–F(6)–Sb(2) = 153.9 (6)°; Sb(3)–F(26) = 1.98 (1) Å, Sb(4)–F(26) = 2.04 (1) Å, Sb(3)–F(26)–Sb(4) = 161.0 (6)°] similar to that of $Sb_2F_{11}^-$ in $TeF_3Sb_2F_{11}$ [Sb–F(bridging) = 1.98 (3) and 2.05 (3) Å, Sb–F(bridging)–Sb = 161 (2)°].[70] The average Sb–F(bridging) and Sb–F(terminal) distances of 2.02 (1) and 1.84 (1) Å, respectively, are similar to those in other structures [e.g.: $TeF_3Sb_2F_{11}$, 2.02 (3) and 1.85 (4) Å;[70] $I_2Sb_2F_{11}$, 2.00 (1) and 1.85 (4) Å[71]]. The equatorial plane of fluorine atoms has an average F(equatorial)–Sb–F(bridging) angle of 85.6 (6)°, which is less than 90° as observed in other structures [e.g.: $TeF_3Sb_2F_{11}$, 85 (1)°; $I_2Sb_2F_{11}$, 86 (2)°). No direct correlation between the Sb–F bond distances and cation–anion contacts is observed.

The average bond distances and angles of the SO_2 unit in $Se_2I_4(AsF_6)_2{\cdot}SO_2$ [average 1.41 (3) Å and 114 (2)°] are similar to those in $Se_6I_2(AsF_6)_4{\cdot}2SO_2$ [average 1.40 (2) Å and 119 (1)°],[6] $Te_6(AsF_6)_4{\cdot}2SO_2$ [average 1.41 (7) Å and 117 (4)°],[33] and solid SO_2 [average 1.43 (2) Å and 119 (2)°].[72] The ordered AsF_6^- anion has an average As–F bond distance of 1.67 (2) Å (cf. 1.70 (1) Å in SeI_3AsF_6).[4] The disordered AsF_6^- anion is modeled by two cocentric AsF_6^- anions with occupancy of 50% each.

Acknowledgment. We thank Dr. F. Grein for assistance with the ab initio calculations and for very helpful discussions and the Natural Sciences and Engineering Research Council (Canada) for financial support.

Supplementary Material Available: A discussion of the complete coordination around the selenium and iodine atoms in $Se_2I_4(Sb_2F_{11})_2$ and $Se_2I_4(AsF_6)_2{\cdot}SO_2$, Figures S1–S6, showing the coordination around various atoms in these compounds, and tables of bond angles for the anion and interionic contacts (Table S1), thermal parameters for $Se_2I_4(Sb_2F_{11})_2$ and $Se_2I_4(AsF_6)_2{\cdot}SO_2$ (Tables S2 and S3, respectively), and crystallographic data (Table S6) (16 pages); tables of observed and calculated structure factors (Tables S4 and S5) (41 pages). Ordering information is given on any current masthead page.

---

(69) Gillespie, R. J. *Molecular Geometry*; Van Nostrand-Reinhold: London, 1972.

(70) Edwards, A. J.; Taylor, P. *J. Chem. Soc., Dalton Trans.* **1973**, 2150.

(71) Davies, C. G.; Gillespie, R. J.; Ireland, P. R.; Sowa, J. M. *Can. J. Chem.* **1974**, *52*, 2048.

(72) Post, B.; Schwartz, R. S.; Frankuchen, I. *Acta Crystallogr.* **1952**, *5*, 372.